Journal of Food and Nutrition Research, 2025, Vol. 13, No. 1, 34-42
Available online at http://pubs.sciepub.com/jfnr/13/1/4
Published by Science and Education Publishing
DOI:10.12691/jfnr-13-1-4

Stachyose Induces Browning Process of White Adipocyte Partly via AMPK Pathway in Vitro

Zhongshan Xiao[1], Zhenglin Chen[2], Siru Chen[2], Xiaoman Yang[3], Tianlin Wang[2,*]

[1]Department of Pharmacy, Puyang Medical College, Puyang, Henan, China
[2]College of Food Science and Technology, Henan Agricultural University, Zhengzhou, China
[3]Puyang People's Hospital, Puyang, Henan, China
*Corresponding author: wangtianlin@henau.edu.cn

Received December 26, 2024; Revised January 28, 2025; Accepted February 04, 2025

Abstract The transformation of white to beige adipocytes is a promising method for the treatment of obesity. The aim of this study was to investigate the effect of stachyose on the regulation of adipocytes browning. The 3T3-L1 preadipocytes and C3H10T1/2 multipotent stem cells were differentiated into mature adipocytes with stachyose (0.5, 2.0 mg/mL). Results showed that the treatment of stachyose significantly decreased intracellular lipid accumulation and increased mitochondrial contents in 3T3-L1 adipocytes and C3H10T1/2 cells. Stachyose, which led to an increase of the relative numbers of UCP1-positive cells, has not only promoted the expression of browning-specific genes and proteins but also induced the phosphorylation of AMPK. Be-sides, the addition of AMPK inhibitor (compound C) has reduced the increase in the protein expression of thermogenesis-related markers induced by stachyose, suggesting that AMPK could affect the stachyose-mediated adipocyte browning process. These results indicate that stachyose has a probable effect on the regulation of adipogenesis and prevention of obesity.

Keywords: *Stachyose, Adipocytes Browning, UCP1, AMPK, Obesity*

Cite This Article: Zhongshan Xiao, Zhenglin Chen, Siru Chen, Xiaoman Yang, and Tianlin Wang, "Stachyose Induces Browning Process of White Adipocyte Partly via AMPK Pathway in Vitro." *Journal of Food and Nutrition Research*. 13, no. 1 (2025): 34-42. doi: 10.12691/jfnr-13-1-4.

1. Introduction

Obesity has been identified as an epidemic disease by the World Health Organisation (WHO). According to the data released by WHO in 2016, more than 1.9 billion adults are overweighted (body mass index (BMI) ≥ 25) and more than 650million are classified as obese (BMI ≥ 30). According to the World Obesity Federation, more than 1 billion people will be obese by 2030 [1]. The cause of obesity is the imbalance between energy intake and expenditure. Excess energy is stored within adipose tissue in the form of triglyceride [2]. There have been convincing evidences shown that obesity is a major risk factor during the development of many common diseases, including type II diabetes, dyslipidaemia, non-alcoholic fatty liver disease, cardiovascular disease, Alzheimer's disease, and even some cancers [3]. Therefore, the demand for developments of effective therapeutic and preventative strategies for combating obesity is urgent.

The dysfunction in adipose tissues plays an important role in the energy homeostasis, and has become the primary target in the treatment of obesity and metabolic disorders. Traditionally, the adipose tissue is divided into brown adipose tissue (BAT) and white adipose tissue (WAT). BAT contains a large number of mitochondria and produces heat by consuming glucose and circulating free fatty acids [4]. The thermogenic function of BAT is mainly activated by the expression of uncoupling protein 1 (UCP1), a protein located in the mitochondrial inner membrane. UCP1 uncouples the oxidative respiratory chain of mitochondria from ATP synthesis with energy dissipated as heat, thereby increasing the total energy consumption [5]. WAT is the major energy storage organ and also an important endocrine organ responsible for regulating biochemical processes such as immunity and metabolic homeostasis [6]. Recently, a subpopulation of cells derived from WAT, known as brown-like adipocytes or beige adipocytes, with phenotypic characteristics and functions closer to brown adipocytes, have been shown to manifest improved thermogenic capacity, increased mitochondrion density, and augmented expression of Ucp1 and other thermogenic genes [7]. Beige adipocytes are generated through WAT browning, a process associated with augmented non-shivering thermogenesis and metabolic capacity [8]. The browning of WAT, which occurs under certain stimulations such as cold exposure, β3-adrenergic receptors, cellular growth factors, and nutritional factors [9], is regarded as a new direction for obesity treatment.

More emerging evidence shows that dietary bioactive compounds and prebiotics [4,10,11] including polyphenols, oligosaccharide or polysaccharides [4,12] have the ability to promote BAT activity as well as induce the browning of WAT [9,10,11]. Stachyose, one of

the non-reducing functional oligosaccharides, widely exists in edible legumes, vegetables, and traditional Chinese medicine [13]. As a non-digestive prebiotics, stachyose can reach the colon without digestion therefore it can interact with gut microbiota directly [14]. Recent studies have indicated that stachyose can promote the proliferation of beneficial intestinal bacteria, inhibit pathogenic bacteria [15], ameliorate type II diabetes [16] and regulate inflammation [14]. It has been reported that stachyose ameliorated metabolic disorders in both HFD mice [17] and diabetic rat [14], indicating a potential role of stachyose in combating obesity. However, whether stachyose can promote the browning of WAT remains unclear. In this study, we have investigated the effect of stachyose on the thermogenic adipocyte differentiation in both 3T3-L1 adipocytes and C3H10T1/2 cells. And the underlying mechanism of stachyose was also explored.

2. Materials and Methods

2.1. Materials

The 3T3-L1 pre-adipocytes and C3H10T1/2 multipotent stem cells used were purchased from American Type Culture Collection (ATCC, Manassas, VA, USA). Triglyceride (TG) detection kits, dexamethasone, insulin, 3-isobutyl-1-methylxanthine and dexamethasone were purchased from Solarbio Science & Technology Co., Ltd (Beijing, China). The indomethacin used was purchased from Aladdin Reagent Co. Ltd. (Shanghai, China) and the 3,3',5-Triiodo-L-thyronine (T3) was purchased from TCI chemicals (TCI, Shanghai, China). MTT was privided by Sigma-Aldrich (St. Louis, MO, USA). MitoTracker® Deep Red FM staining reagent and lysis buffer was purchased from Beyotime Biotech. Inc. (Jiangsu, China). Antibodies against UCP1 (#ab10983), SIRT1 (#ab110304), PGC1α (#ab54481), PRDM16 (#ab106410) were obtained from Abcam (Cambridge, MA, USA). Antibodies against t-AMPK (#5832S) and p-AMPK (#2535S) were purchased from Cell Signaling Technology (Beverly, MA, USA).

2.2. Cell culture, Differentiation and Treatment

The 3T3-L1 pre-adipocytes and C3H10T1/2 multipotent stem cells were grown in Dulbecco's Modified Eagle's Medium (DMEM) (Solarbio, Beijing, China), supplemented with 10% fetal bovine serum (BioInd, Kibbutz Beit, IL) and 1% penicillin streptomycin (HyClone, UT, USA). Cells were then placed in a humidified 5% CO2 incubator at 37°C. To further induced their differentiation, cells were inoculated in 6-well culture plates to reach 70-80% confluence. Then, 3T3-L1 preadipocytes and C3H10T1/2 multipotent stem cells were cultured for 2 days in differentiation medium containing 10 μg/mL insulin, 1.0 μM dexamethasone, 0.125 mM indomethacin, 10 nM T3 and 0.5 mM 3-isobutyl-1-methylxanthine. After that, cells were transferred to growth medium containing 10 μg/mL insulin and 10 nM T3 for another 6 days. During 8 days of the differentiation period, cells were devided into 3 groups, according to the level of stachyose in the incubation medium (0, 0.5 and 2.0 mg/mL correspondingly).

2.3. Cell Viability Assay

MTT assay was conducted to examine the cell viability. Cells were inoculated into 96-well plates and stachyose at 0.01 – 16.00 mg/mL were added to the medium for 24 h. After incubation, MTT solution (5 mg/mL) was added and cells were incubated at 37 °C for another 4 h. Then the medium containing MTT was removed and 180 μL of DMSO solution was added into each well to solubilize cells. The absorbance of each well was detected using a microplate reader (Bio-Rad, Hercules, CA, USA) at 570 nm.

2.4. Oil Red O staining Assay and Triglyceride Content Determination

The lipid accumulation was measured by Oil Red O staining and TG content measurments. The Oil Red O solution was prepared as described previously [18]. After differentiation, the mature adipocytes were washed twice using PBS and fixed with 4% paraformaldehyde for 10 min. Then the cells were washed with PBS twice and treated with a filtered 0.3% Oil Red O solution to stain for 20 min. After staining, the cells were washed three times with distilled water or PBS. Subsequently, the cells were observed and photographed under an optical microscope (Axiomager, Zeiss, Germany) at 200× magnification. Isopropanol was added to the cells for 20 min at room temperature to dissolve lipid droplets. The absorbance was measured at 510 nm using a microplate reader (Bio-Rad, Hercules, CA, USA). Thereafter, cells were transferred into a 96-well culture plate and placed in an Enzyme-linked Immunosorbent Assay (ELISA) reader to detect the absorbance value at 510 nm. The TG levels after stachyose treatment were measured with commercial TG colorimetric essay kit following the manufacturer's instructions.

2.5. Ucp1 Immunofluorescence and Mitochondrial Content Analysis

The differentiated mature adipocytes were washed using PBS for three times and then stained by MitoTracker® Deep Red FM at 200 nM for 30 min. The nucleus was stained with Hoechst 33342 (Beyotime Biotech, Jiangsu, China) for 10 min. At the end of the staining, cells were rinsed 3 times with PBS. Immunofluorescence for UCP1 was performed as follows: cells were blocked in a DMEM-based blocking buffer supplemented with 10% FBS for 1 hour at room temperature. Following this, a polyclonal antibody against UCP1 (Sigma, U6382) was applied at a dilution of 1:500 in the blocking buffer and incubated overnight at 4 °C. Next, the cells were washed with PBS and incubated with an Alexa F488-conjugated secondary antibody against IgG (Life Technologies, Molecular Probes, A21206) at a dilution of 1:500. This incubation step lasted for 2 hours at room temperature. After the final washes with PBS, the cells were mounted using ProLong Gold Antifade Reagent (Life Technologies, Molecular Probes).

Images containing *Ucp1* immunofluorescence and MitoTracker staining were observed and pictured by laser confocal microscope.

Table 1. Primer sequences used for RT-PCR

Gene	Forward Sequence (5'-3')	Reverse Sequence (5'-3')
Ucp1	ACTGCCACACCTCCAGTCATTH	CTTTGCCTCACTCAGGATTGGH
Pgc1α	CCCTGCCATTGTTAAGACCA	TGCTGCTGTTCCTGTTTTCH
Prdm16	CAGCACGGTGAAGCCATTCA	GCGTGCATCCGCTTGTGH
Cidea	ATCACAACTGGCCTGGTTACG	TACTACCCGGTGTCCATTTCT
Cox7a	TTCGAGAACCGAGTAGCTGAGAAC	CTGTTGCACCGCCCTTCAC
Cyt C	CCAAATCTCCACGGTCTGTTC	ATCAGGGTATCCTCTCCCCAG
Tfam	GAGGCCAGTGTGAACCAGTGA	GTAGTGCCTGCTGCTCCTGA
GAPDH	GTAACCCGTTGAACCCCATT	CCATCCAATCGGTAGTAGCGA

2.6. Real-time PCR Analysis

Real-time PCR was conducted as described in [19]. After incubation, the total cellular RNA was extracted using a total RNA isolation kit (Tiangen, Beijing, China) in accordance with the manufacturer's instructions. Subsequently, total RNA was reverse-transcribed into the cDNA PrimeScript RT reagent kit (Tiangen, Beijing, China). The resultant cDNA was amplified by the RT-PCR instrument (Thermo Fisher, MA, USA). GAPDH was used as a control to normalize the differences in mRNA levels. The primer sequences used in this study are listed in the supporting information Table S1. The expression levels of each gene were quantified using that comparative cycle threshold (2–ΔΔCt) method.

2.7. Western Blot Analysis

The cells were treated with cell lysis buffer containing protease inhibitor cocktail. The mixture was then disrupted by ultrasonic treatment and centrifuged at 4°C for 15 min.

The BCA protein assay kit was used to determine total protein concentrations. The cell lysates (30 μg of protein) were subjected to 10% sodium dodecyl sulfate-polyacrylamide gel electrophoresis (SDS-PAGE), transferred to polyvinylidene difluoride (PVDF) membranes (Millipore Corporation, Billerica) and then blocked by 5% skimmed milk for 1 h. The PVDF membrane was incubated with primary antibodies overnight at 4 °C. Then, the membrane was washed with 1×TBST for five minutes and incubated with peroxidase conjugated secondary antibody for 1 h. After washing with 1×TBST five times, immunoblots were developed using enhanced chemiluminescence detection reagents (CWBio, Beijing, China) and images were detected using a chemiluminescence detection system (Beyotime Biotech, Jiangsu, China). Protein levels were normalized to those of β-actin. The intensity of bands was quantified using the software ImageJ 1.47v (NIH, Bethesda, MD).

2.8. Statistical Analyses

All values were presented as the as mean ± standard deviation (SD). Statistical analysis was performed with one-way ANOVA followed by Tukey's test. Differences were considered statistically significant at $P < 0.05$. All experiments were performed independently and on at least three occasions.

3. Results

3.1. Effect of Stachyose on the Cell Viability of 3T3-L1 Adipocytes and C3H10T1/2 Cells

To investigate the effects of stachyose on the cell viability, a series of concentrations of stachyose were tested on 3T3-L1 adipocytes and C3H10T1/2 cells by MTT analysis. The results showed that intervention of stachyose (0.01-2.00 mg/mL) for 48 h had no significant effect on cell viability in 3T3-L1 adipocytes and C3H10T1/2 cells. And a significant decrease in cell viability was observed after stachyose intervention at 8.00 or 16.00 mg/mL in 3T3-L1 adipocytes (Figure 1A) and C3H10T1/2 cells (Figure 1B), compared to the control group. Therefore, the concentrations of 0.50 and 2.00 mg/mL of stachyose were chosen for the following experiments.

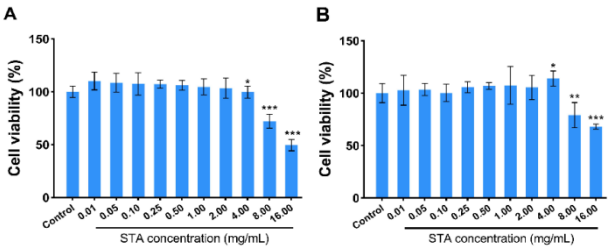

Figure 1. Effect of stachyose on the cell viability of 3T3-L1 pre-adipocytes and C3H10T1/2 multipotent stem cells. Cell viability of 3T3-L1 pre-adipocytes (A) and C3H10T1/2 multipotent stem cells (B) were assessed after stachyose treatment at various concentrations for 48 hours by the MTT assay. Data are expressed as mean ± SD (n = 6). * $P < 0.05$, ** $P < 0.01$, and *** $P < .001$ versus the control group

3.2. Stachyose Alleviated Intracellular Lipid Accumulation in 3T3-L1 Adipocytes and C3H10T1/2 Cells

Oil Red O staining was performed and TG content were measured to investigate the effect of stachyose on the lipid accumulation in 3T3-L1 adipocytes and C3H10T1/2 cells. As shown in Figure 2A and 2C, stachyose-treated groups resulted noticeably smaller lipid droplets compared to the control group in 3T3-L1 adipocytes and C3H10T1/2 cells. The semi-quantitative analysis of Oil red O staining showed that stachyose at 0.5 mg/mL and 2.0 mg/mL significantly reduced the lipid accumulation of C3H10T1/2 cells (Figure 2B). A significant reduction in absorbance compared to the control group was observed in the stachyose treatment group at a concentration of 2.0 mg/mL in 3T3-L1 adipocytes (Figure 2D). Besides, stachyose intervention also decreased the level of TG content in both 3T3-L1 adipocytes and C3H10T1/2 cells (Figure 2E and 2F).

3.3. Stachyose Enhanced Mitochondrial Biogenesis in 3T3-L1 Adipocytes and C3H10T1/2 Cells

To investigate the effect of stachyose on the mitochondrial biogenesis, the cells were stained with MitoTracker Deep Red to measure the mitochondria abundance. Results showed that the red fluorescence intensity was significantly increased in 3T3-L1 adipocytes (Figure 3A and 3B) and C3H10T1/2 cells (Figure 3C and 3D) after stachyose treatment, indicating an elevation in mitochondrial content. Moreover, stachyose up-regulated the mRNA expression of mitochondria biogenesis-related genes (Cox7a, Cyt C, and Tfam) in both 3T3-L1 adipocytes (Figure 3E) and C3H10T1/2 cells (Figure 3F). These findings indicates that the intervention of stachyose increased the mitochondrial biogenesis.

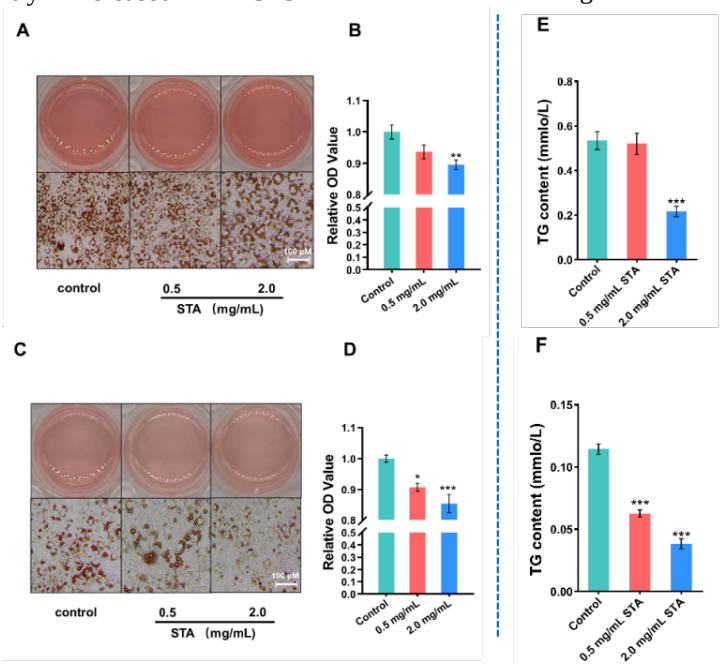

Figure 2. Effects of stachyose on the intracellular lipid accumulation in 3T3-L1 adipocytes and C3H10T1/2 cells. Typical pictures were observed with light microscope after Oil Red O staining in 3T3-L1 adipocytes (A) and C3H10T1/2 adipocytes (C). (×80 magnification , scale bar=200 μm). Semi-quantitative analysis of Oil Red O stained 3T3-L1 adipocytes (B) and C3H10T1/2 cells (D). The level of TG content in 3T3-L1 adipocytes (E) and C3H10T1/2 cells (F). Data are expressed as mean ± SD (n = 6). * P < 0.05 , ** P < 0.01, and *** P < .001 versus the control group

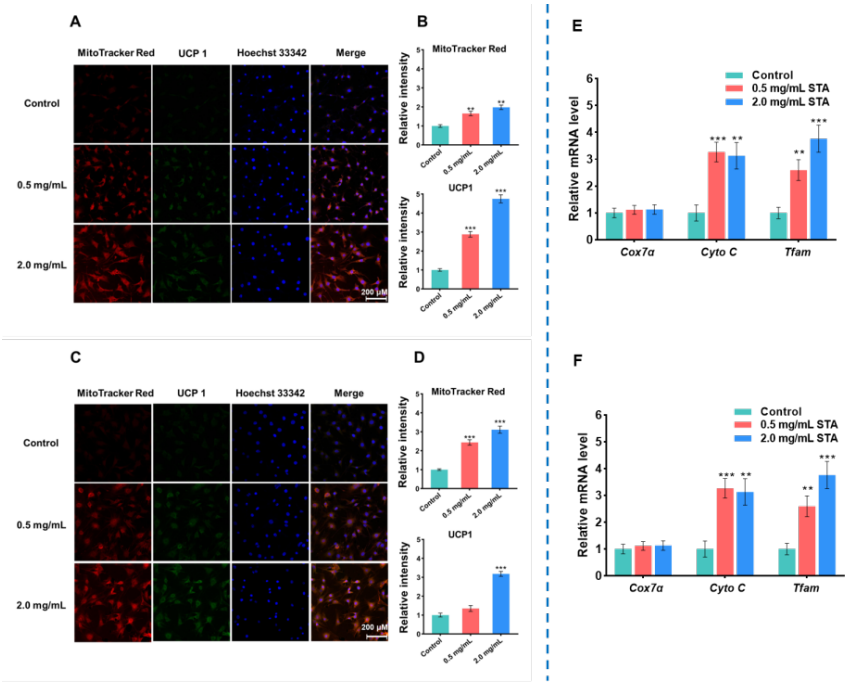

Figure 3. Effects of stachyose on the mitochondrial biogenesis in 3T3-L1 adipocytes and C3H10T1/2 adipocytes. 3T3-L1 adipocytes (A) and C3H10T1/2 adipocytes(C). Images were analyzed with a fluorescence microscope (×200 magnification). Quantitative data for MitoTracker Red and UCP1 immunofluorescence staining intensity in 3T3-L1 adipocytes (B) and C3H10T1/2 adipocytes (D). Relative mRNA expression of mitochondrial biogenesis-related genes were measured by RT-PCR in 3T3-L1 adipocytes (E) and C3H10T1/2 adipocytes (F). Data are expressed as mean ± SD (n = 4). * P < 0.05 , ** P < 0.01, and *** P < .001 versus the control group

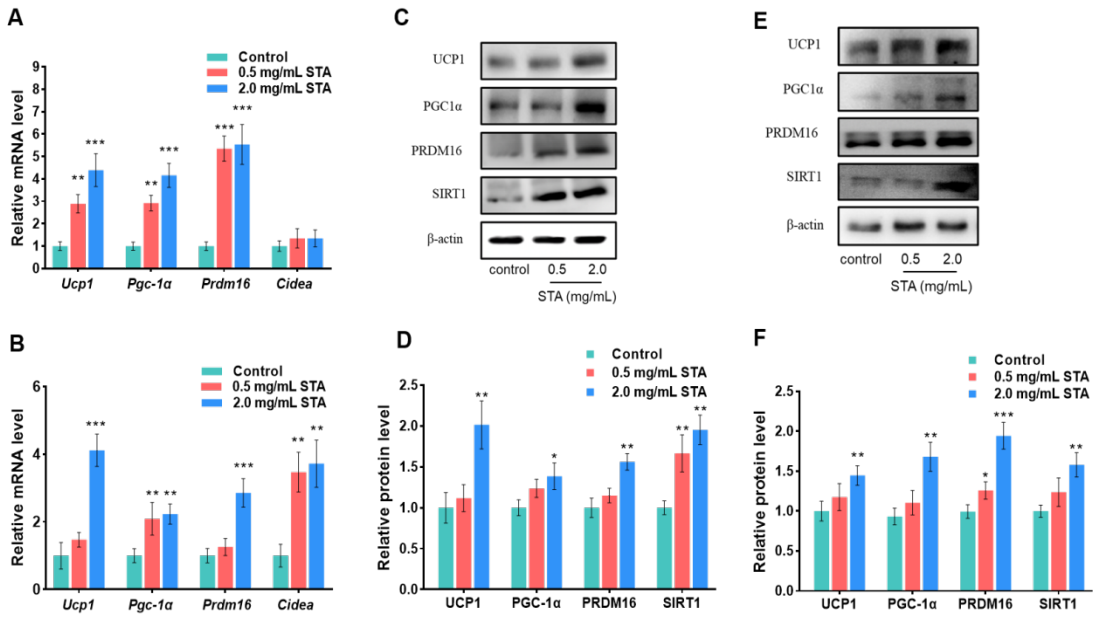

Figure 4. Effect of stachyose on the expression of browning-specific genes and proteins in 3T3-L1 adipocytes and C3H10T1/2 adipocytes. The mRNA expression levels of browning-specific genes were measured by RT-PCR in 3T3-L1 adipocytes (A) and C3H10T1/2 adipocytes (B). The protein expression of UCP1, PGC1α, PDRM16 and SIRT1 were measured by western blot in 3T3-L1 adipocytes (C and D) and C3H10T1/2 adipocytes (E and F). Data are expressed as mean ± SD (n = 3). * P < 0.05 , ** P < 0.01, and *** P < .001 versus the control group

3.4. Stachyose Promoted the Expression of Browning-specific Genes and Proteins in 3T3-L1 Adipocytes and C3H10T1/2 Cells

Then, the effects of stachyose on the expression of browning-specific genes and proteins were further determined in 3T3-L1 adipocytes and C3H10T1/2 cells. Stachyose intervention at 0.5 mg/mL or 2.0 mg/mL demonstrated varying degrees of enhancement in the expression of Ucp1, Pgc1α, Prdm16, Sirt1 in 3T3-L1 adipocytes (Figure 4A) and C3H10T1/2 cells (Figure 4B). When the concentration of stachyose was at 2.0 mg/mL, the UCP1, PGC1α, PRDM16, SIRT1 expression in 3T3-L1 adipocytes were raised up to 2.01 fold, 1.38 fold, 1.56 fold, 1.95 fold, respectively (Figure 4C and 4D), while raised the UCP1, PGC1α, PRDM16 and SIRT1 expression in C3H10T1/2 cells up to 1.45 fold, 1.68 fold, 1.94 fold, 1.58 fold (Figure 4E and 4F). The above data demonstrated that the stachyose treatment promoted the expression of UCP1 and other browning markers, and indeced the formation of beige cells as a result.

3.5. Stachyose Improved Degree of AMPK Phosphorylation in 3T3-L1 Adipocytes and C3H10T1/2 Cells

To investigate the effect of stachyose on the degree of AMPK phosphorylation in 3T3-L1 adipocytes and C3H10T1/2 cells, the ratio of p-AMPK/t-AMPK was analysed by western blot. Results showed a higher ratio of p-AMPK/t-AMPK in the stachyose-treated group, where the stachyose treatment upregulated the phosphorylation of AMPK in 3T3-L1 adipocytes (Figure 5A) and C3H10T1/2 cells (Figure 5C), compared with the control group. Furthermore, the band intensity that in the 2.0 mg/mL stachyose treatment group was significantly higher than that in the control group in 3T3-L1 adipocytes (Figure 5B) and C3H10T1/2 cells (Figure 5D).

3.6. Stachyose-mediated Thermogenesis is Partially Dependent on the Activation of AMPK in 3T3-L1 Adipocytes and C3H10T1/2 Cells

To investigate whether stachyose-mediated thermogenesis could be associated with AMPK signaling pathway, the AMPK inhibitor compound C was added to stachyose-treated differentiation medium. Stachyose treatment alone led to a significant increase in the expression of UCP1, PGC1α, PRDM16 and the ratio of p-AMPK/t-AMPK in 3T3-L1 adipocytes (Figure 6A and 6B) and C3H10T1/2 cells (Figure 6C and 6D), compared to the control group. On the contrary, in the presence of compound C, the increase in the expression of UCP1, PGC1α, PRDM16 and the ratio of p-AMPK/t-AMPK mediated by stachyose was significantly inhibited. These findings suggested that the thermogenic effects induced by stachyose in 3T3-L1 adipocytes and C3H10T1/2 cells was partially dependent on the activation of AMPK.

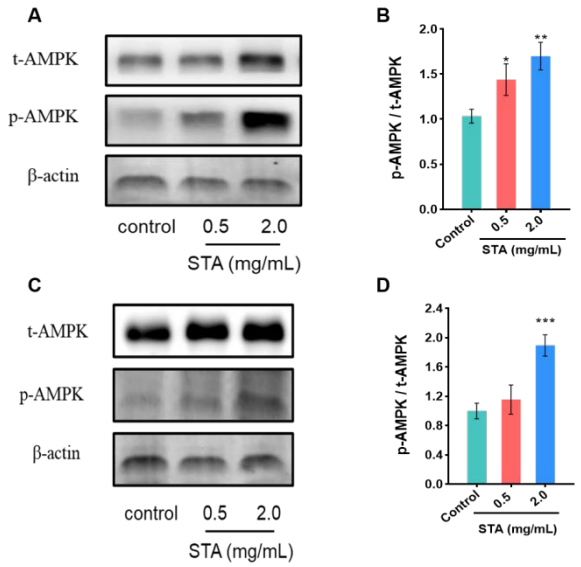

Figure 5. Effect of stachyose on the phosphorylation of AMPK in 3T3-L1 adipocytes and C3H10T1/2 cells. The phosphorylation of AMPK was analysed by western blot in 3T3-L1 adipocytes (A and B) and C3H10T1/2 adipocytes (C and D). Data are expressed as mean ± SD (n = 3). *P < 0.05 , ** P < 0.01, and *** P < .001 versus the control group

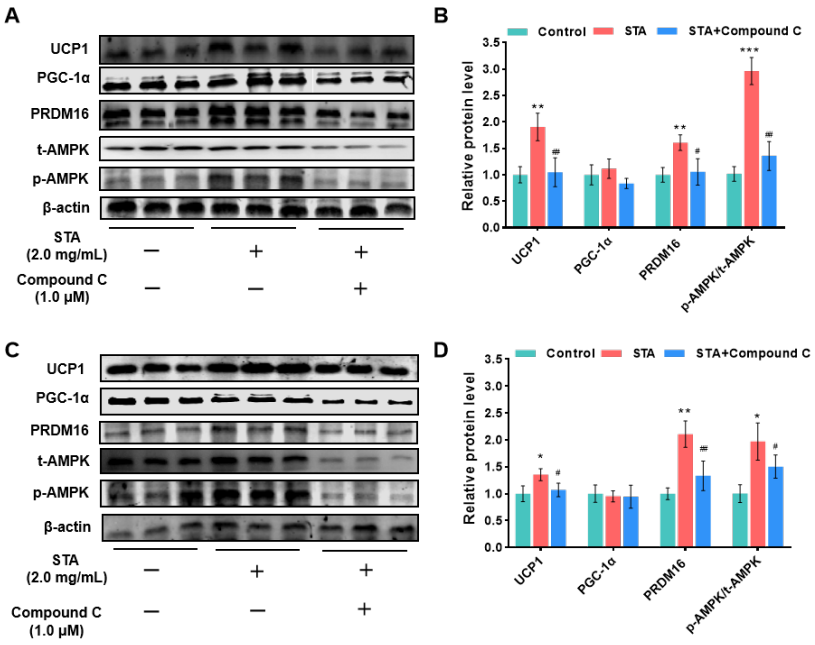

Figure 6. Effect of compound C on the AMPK signaling pathway in stachyose-treated 3T3-L1 adipocytes and C3H10T1/2 cells. The protein expression of UCP1, PGC1α, PDRM16, p-AMPK and t-AMPK were measured by western blot in 3T3-L1 adipocytes (A and B) and C3H10T1/2 adipocytes (C and D). Data are expressed as mean ± SD (n = 3). * P < 0.05 , ** P < 0.01, and *** P < .001 versus the control group; # P<0.05, ## P < 0.01, ### P <0.001 versus stachyose-treated group

4. Discussion

Inducing the browning of white adipose tissue (WAT) to exhibit the thermogenic phenotype is a promising way for the treatment of obesity [6]. In this study, the effect of stachyose on the brown remodeling of WAT in 3T3-L1 pre-adipocytes and C3H10T1/2 multipotent stem cells was investigated. Our results indicated that stachyose not only effectively alleviated the intracellular lipid accumulation in 3T3-L1 adipocytes and C3H10T1/2 cells, but also promoted the mitochondrial biogenesis and increased the gene and protein expression of thermogenic markers. In addition, the activation of thermogenesis mediated by stachyose was closely related to AMPK pathway in 3T3-L1 adipocytes and C3H10T1/2 cells. Collectively, our data imply that stachyose induced the browning of WAT, thus providing a potential strategy for the prevention of obesity and its related metabolic disorders. The expansion of adipose tissue in obesity can be attributed to the augmentation in both the number (hyperplasia) and size of adipocytes [20]. This hyperplasia is thought to arise from the recruitment of preadipocytes from pluripotent stem cells located within the vascular stroma of adipose tissue [21]. It is followed by the mitotic clonal expansion that takes place during preadipocyte differentiation [22]. The 3T3-L1 cell line is one of the most widely characterized and extensively studied cell models for preadipocyte

differentiation [23], which is derived from disaggregated mouse embryo [24]. The C3H10T1/2 cell line is a valuable model system for studying the commitment of mesenchymal stem cells (MSCs) to the adipocyte lineage [25]. This cell line represents an earlier stage of development compared to the 3T3-L1 line [26,27], which is isolated from 14 to 17-day-old C3H mouse embryos [28]. Stachyose and four other oligosaccharides (galacto-oligosaccharides, xylo-oligosaccharides, inulin and resistant dextrin) at 0.125, 0.25, 0.5 mg/mL exerted anti-inflammatory effect in LPS-stimulated RAW264.7 macrophages in a dose-dependent manner, whereas stachyose was most effective in vitro [29]. Moreover, in the range of 0.4-3.2 mg/mL, stachyose treatment did not exhibit any inhibitory effects on the viability of Caco-2 cells[30]. Consistent with these findings, our study also showed that stachyose at 0.5 or 2.0 mg/mL treatment significantly promoted the formation of beige cells with no toxicity in 3T3-L1 adipocytes and C3H10T1/2 cells.

Mounting evidence supporting the promising potentials of functional oligosaccharides in the prevention of obesity by regulating adipocyte differentiation. Low molecular chitosan oligosaccharide significantly decreased intracellular lipid accumulation and inhibited the differentiation of 3T3-L1 preadipocytes into white adipocytes, thereby showing the anti-obesity effects [31]. Raffinose, an oligosaccharide isolated from Costus speciosus, inhibited lipid accumulation by the activation of fatty acid oxidation with the suppression of lipogenesis in 3T3-L1 adipocytes [32]. Xylo-oligosaccharides exhibited notable effects on the reduction of body weight gain as well as the improvement of serum lipid profile in obese rats [33]. Mannan oligosaccharides have demonstrated a dose-dependent mitigation of weight gain and metabolic syndrome induced by high-fat diet, and coffee-derived mannan oligosaccharides have also shown efficacy in promoting weight loss in overweight men [34]. Stachyose, a widely recognized and commonly used oligosaccharide, has been extensively incorporated into nutritional recommendations for the management of metabolic syndromes [35]. Research has indicated that stachyose plays a significant role in improving gut function and regulating glucose metabolism, which has the potential to improve type II diabetes [16]. Consistent with the aforementioned findings, we observed that the stachyose-treated groups exhibited a significant reduction in intracellular lipid accumulation and TG content in 3T3-L1 adipocytes and C3H10T1/2 cells.

Mitochondria, serving as the powerhouse of cells, play a crucial role in energy production by supplying over 95% of the ATP required for cellular metabolism [31]. Mitochondrial biogenesis is a process associated with the increase in mitochondrial mass and mtDNA copy number, which occurs during the transformation of beige cells [36]. In our study, stachyose promoted mitochondrial biogenesis by increasing mitochondrial abundance and up-regulating gene expression of mitochondrial biogenesis-related markers including Cox7a, Cyt C, and Tfam. PGC1α is a critical regulator of mitochondrial energy metabolism[37], which stimulates the mitochondrial biogenesis by activating various transcription factors, and indirectly promote the level of Tfam (mitochondrial transcription factor A)[38]. Cytochrome C (Cyt C) plays a key role in mitochondrial oxidative phosphorylation. Cytochrome oxidase (COX), such as COX7a, is an endogenous enzyme located at the distal end of the mitochondrial respiratory chain, exhibiting high expression in brown adipocytes [39]. Previous research has shown that stachyose elevated the expression of apoptotic proteins to cause the loss of inner mitochondrial membrane potential, leading to the up-regulation of Cyt C expression [30]. The ganglioside GM1 oligosaccharide regulated mitochondrial function by increasing mitochondrial density and an enhanced mitochondrial activity in wild-type Neuro2a cells [39,40]. Alginate oligosaccharide improved mitochondrial biogenesis and maintained the mitochondrial integrity to prevent cardiac dysfunction in D-galactose-induced C57BL/6J ageing mice [41]. Consistent with theses results, our results also revealed that stachyose treatment induced an increase in expression of mitochondria biogenesis-related genes and mitochondria abundance in 3T3-L1 adipocytes and C3H10T1/2 cells.

During the browning process, WAT shows thermogenic proteins expressions, such as PRDM16, PGC1α, UCP1, which have vital roles in the development and function of adipocyte precursor cell lineages as well as beige or brown adipocytes [42]. UCP1 is located within the mitochondrial inner membrane and is involved in uncoupling respiration in BAT by increasing glucose and free fatty acid oxidation, thereby promoting heat production through mitochondrial respiration [43]. PR domain containing 16 (PRDM16) is an essential mediator for the adipose tissue metabolism [44], serving as a transcription factor that governs the browning and thermogenesis of adipocytes, and controls the fate and differentiation of brown and beige fat cells [45,46]. Evidence suggests that oligosaccharides, such as chitosan oligosaccharide [47] and epilactose [48] induce an upregulation in expression browning-specific proteins containing UCP1, PRDM16, PGC1α. Consistent with these findings, our results showed that stachyose treatment increased the expression of browning-specific genes and proteins in 3T3-L1 adipocytes and C3H10T1/2 cells. These results indicated that stachyose effectively promote the browning of w1adipose tissue in vitro.

AMPK functions as a pivotal regulator of energy sensing and homeostasis [49]. Activation of AMPK through phosphorylation promotes catabolic pathways, such as fatty acid oxidation, while concurrently inhibiting energy-consuming pathways [50]. AMPK activity is subject to comprehensive regulation by multiple upstream signals, thus positioning AMPK as a central hub utilized by cells to synchronize their metabolism with specific energy requirements [51]. In addition, AMPK phosphorylate and inhibit transcription factors involved in lipogenesis, such as SREBP1, thereby limiting lipid synthesis and promoting fatty acid oxidation for energy supply [52].Regulation of the AMPK phosphorylation by dietary bioactive compounds promotes differentiation and recruitment of beige adipocytes. SIRT1 [sirtuin (silent mating type information regulation 2 homologue) 1] is a cellular fuel sensor coexisting with AMPK, with both molecules mutually regulating each other and exhibiting similar roles in various biochemical processes, including cellular energy metabolism [53]. Previous studies have revealed that fructo-oligosaccharide [54] and chitosan

oligosaccharides [55] induce AMPK activation via the CAsR signaling pathway. Our results suggested that the ratio of p-AMPK/t-AMPK was significantly increased after stachyose treatment versus control group in 3T3-L1 adipocytes and C3H10T1/2 cells. Compound C, also known as dorsomorphin, is a cell-permeable inhibitor of AMPK [56,57], and widely employed in various cellular, biochemical, and in vivo experiments [58]. To investigate whether stachyose-induced browning of WAT is mediated through the AMPK pathway, we examined the expression of browning-specific proteins with or without compound C in 3T3-L1 adipocytes and C3H10T1/2 cells. Our results revealed that the expression levels of browning-specific proteins were significantly lower after treatment of stachyose plus compound C compared to the stachyose-treated group in 3T3-L1 adipocytes and C3H10T1/2 cells. These results indicated that stachyose-mediated browning of adipose tissue is partly dependent on the activation of AMPK. However, the role of stachyose in the promotion of WAT browning needs to be further investigated in vivo, which can provide more data and basis for the use of stachyose in obesity prevention and treatment.

5. Conclusions

In summary, our results supported that stachyose promotes adipocyte browning, and this effect was mediated through the AMPK signaling pathway. Stachyose were found to improve mitochondrial biogenesis and lipid accumulation in both 3T3-L1 adipocytes and C3H10T1/2 cells. It induced a brown-like adipocyte phenotype by upregulating the expression of UCP1, along with other thermogenic genes and beige cell markers. Additionally, it remarkable promote the t-AMPK phosphorylation in both 3T3-L1 adipocytes and C3H10T1/2 cells. Therefore, stachyose may have significant potential and value as a functional food excipient for the treatment and prevention of obesity.

Acknowledgments: This work was supported by the National Natural Science Foundation of China (NO. 32101966), 2022 Henan postgrad-uate joint training base project (NO. YJS2022JD16), and the Program for Innovative Research Team (in Science and Technology) in university of Henan Province (NO. 23IRTSTHN023).

Conflicts of Interest: The authors declare no conflict of interest.

References

[1] Di Ciaula, A.; Portincasa, P. Contrasting obesity: is something missing here? *Internal and Emergency Medicine.* **2024**, *19*, 265-269.

[2] Andolfi, C.; Fisichella, P.M. Epidemiology of Obesity and Associated Comorbidities. *Journal of Laparoendoscopic & Advanced Surgical Techniques.* **2018**, *28*, 919–924.

[3] O'Neill, S.; O'Driscoll, L. Metabolic syndrome: a closer look at the growing epidemic and its associated pathologies. *Obesity Reviews.* 2015, 16, 1-2.

[4] Suchacki, K.J.; Stimson, R.H. Nutritional Regulation of Human Brown Adipose Tissue. *Nutrients.* **2021**, *13*, 1748.

[5] Merlin, J.; Evans, B.A.; Dehvari, N.; Sato, M.; Bengtsson, T.; Hutchinson, D.S. Could Burning Fat Start with a Brite Spark? Pharmacological and Nutritional Ways to Promote Thermogenesis. *Molecular Nutrition Food Res.* **2016**, *60*, 18–42.

[6] Peirce, V.; Carobbio, S.; Vidal-Puig, A. The different shades of fat. *Nature*. **2014**, 510, 76-83.

[7] Xue, S.W.; Lee, D.R.; Berry, D.C. Thermogenic adipose tissue in energy regulation and metabolic health. *Frontiers in Endocrinology*. **2023**, 14, 1150059.

[8] Machado, S.A.; Pasquarelli-do-Nascimento, G.; Da Silva, D.S.; Farias, G.R.; De Oliveira Santos, I.; Baptista, L.B.; Magalhães, K.G. Browning of the White Adipose Tissue Regulation: New Insights into Nutritional and Metabolic Relevance in Health and Diseases. *Nutr Metab (Lond).* **2022**, *19*, 61.

[9] Harms, M.; Seale, P. Brown and Beige Fat: Development, Function and Therapeutic Potential. *Nat Med.* **2013**, *19*, 1252–1263.

[10] Yoneshiro, T.; Matsushita, M.; Saito, M. Translational Aspects of Brown Fat Activation by Food-Derived Stimulants. In *Brown Adipose Tissue*; Pfeifer, A., Klingenspor, M., Herzig, S., Eds.; Handbook of Experimental Pharmacology; Springer International Publishing: Cham, **2018**; Vol. 251, pp. 359–379 ISBN 978-3-030-10512-9.

[11] Ono, K.; Tsukamoto-Yasui, M.; Hara-Kimura, Y.; Inoue, N.; Nogusa, Y.; Okabe, Y.; Nagashima, K.; Kato, F. Intragastric Administration of Capsiate, a Transient Receptor Potential Channel Agonist, Triggers Thermogenic Sympathetic Responses. *Journal of Applied Physiology*. **2011**, *110*, 789–798.

[12] Valente, A.; Carrillo, A.E.; Tzatzarakis, M.N.; Vakonaki, E.; Tsatsakis, A.M.; Kenny, G.P.; Koutedakis, Y.; Jamurtas, A.Z.; Flouris, A.D. The Absorption and Metabolism of a Single L-Menthol Oral versus Skin Administration: Effects on Thermogenesis and Metabolic Rate. *Food and Chemical Toxicology*. **2015**, *86*, 262–273.

[13] Li, W.; Li, Z.; Han, X.; Huang, D.; Lu, Y.; Yang, X. Enhancing the Hepatic Protective Effect of Genistein by Oral Administration with Stachyose in Mice with Chronic High Fructose Diet Consumption. *Food Funct.* **2016**, *7*, 2420–2430.

[14] Liu, G.; Bei, J.; Liang, L.; Yu, G.; Li, L.; Li, Q. Stachyose Improves Inflammation through Modulating Gut Microbiota of High‐Fat Diet/Streptozotocin‐Induced Type 2 Diabetes in Rats. *Molecular Nutrition Food Res.* **2018**, *62*, 1700954.

[15] Li, T.; Lu, X.; Yang, X. Stachyose-Enriched α-Galacto-Oligosaccharides Regulate Gut Microbiota and Relieve Constipation in Mice. *J. Agric. Food Chem.* **2013**, *61*, 11825–11831.

[16] Yan, T.; Liu, T.; Shi, L.; Yan, L.; Li, Z.; Zhang, X.; Dai, X.; Sun, X.; Yang, X. Integration of Microbial Metabolomics and Microbiomics Uncovers a Novel Mechanism Underlying the Antidiabetic Property of Stachyose. *Journal of Functional Foods.* **2023**, *102*, 105457.

[17] Liu, Y.; Li, T.; Alim, A.; Ren, D.; Zhao, Y.; Yang, X. Regulatory Effects of Stachyose on Colonic and Hepatic Inflammation, Gut Microbiota Dysbiosis, and Peripheral $CD4^+$ T Cell Distribution Abnormality in High-Fat Diet-Fed Mice. *J. Agric. Food Chem.* **2019**, *67*, 11665–11674.

[18] Shepherd, P.R.; Gnudi, L.; Tozzo, E.; Yang, H.; Leach, F.; Kahn, B.B. Adipose Cell Hyperplasia and Enhanced Glucose Disposal in Transgenic Mice Overexpressing GLUT4 Selectively in Adipose Tissue. *Journal of Biological Chemistry.* **1993**, *268*, 22243–22246.

[19] Lee, S.G.; Lee, Y.J.; Jang, M.-H.; Kwon, T.R.; Nam, J.-O. Panax Ginseng Leaf Extracts Exert Anti-Obesity Effects in High-Fat Diet-Induced Obese Rats. *Nutrients.* **2017**, *9*, 999.

[20] Li, T.; Du, M.; Wang, H.; Mao, X. Milk Fat Globule Membrane and Its Component Phosphatidylcholine Induce Adipose Browning Both in Vivo and in Vitro. *The Journal of Nutritional Biochemistry.* **2020**, *81*, 108372.

[21] Yu, Z.K.; Wright, J.T.; Hausman, G.I. Preadipocyte Recruitment in Stromal Vascular Cultures After Depletion of Committed Preadipocytes by Immunocytotoxicity. *Obesity Research.* **1997**, *5*, 9–15.

[22] Tang, Q.-Q.; Otto, T.C.; Lane, M.D. Mitotic Clonal Expansion: A Synchronous Process Required for Adipogenesis. *Proc. Natl. Acad. Sci. U.S.A.* **2003**, *100*, 44–49.

[23] Cornelius, P.; MacDougald, O.A.; Lane, M.D. Regulation of adipocyte development. *Annual review of nutrition*. **1994**, 14(1): 99-129.

[24] MacDougald, O.A; Lane, M.D. Transcriptional regulation of gene expression during adipocyte differentiation. *Annual review of biochemistry*. **1995**, 64(1): 345-373.

[25] Um, J.-H.; Park, S.-J.; Kang, H.; Yang, S.; Foretz, M.; McBurney, M.W.; Kim, M.K.; Viollet, B.; Chung, J.H. AMP-Activated Protein Kinase–Deficient Mice Are Resistant to the Metabolic Effects of Resveratrol. *Diabetes*. **2010**, *59*, 554–563.

[26] Taylor, S.M; Jones, P.A. Multiple new phenotypes induced in 10T1/2 and 3T3 cells treated with 5-azacytidine. *Cell*. 1979 Aug, 17(4):771-9.

[27] Bowers, R.R.; Kim, J.W.; Otto, T.C.; Lane, M.D. Stable Stem Cell Commitment to the Adipocyte Lineage by Inhibition of DNA Methylation: Role of the BMP-4 Gene. *Proc. Natl. Acad. Sci. U.S.A.* **2006**, *103*, 13022–13027.

[28] Reznikoff, C.A.; Brankow, D.W.; Heidelberger, C. Establishment and Characterization of a Cloned Line of C3H Mouse Embryo Cells Sensitive to Postconfluence Inhibition of Divisio. *Cancer Research*. **1973**, *33*

[29] Jiang S., Li Q, Han S, et al. Study on the Anti‐inflammatory Effect of Stachyose by Inhibiting TLR4/NF‐κB Signaling Pathway in Vitro and in Vivo. C*linical and Experimental Pharmacology and Physiology*. **2023**, *50(7)*, 573-582.

[30] Huang, G.; Mao, J.; Ji, Z.; Ailati, A. Stachyose-Induced Apoptosis of Caco-2 Cells via the Caspase-Dependent Mitochondrial Pathway. *Food Funct.* **2015**, *6*, 765–771.

[31] Lee, J.-Y.; Kim, T.Y.; Kang, H.; Oh, J.; Park, J.W.; Kim, S.-C.; Kim, M.; Apostolidis, E.; Kim, Y.-C.; Kwon, Y.-I. Anti-Obesity and Anti-Adipogenic Effects of Chitosan Oligosaccharide (GO2KA1) in SD Rats and in 3T3-L1 Preadipocytes Models. *Molecules*. **2021**, *26*, 331.

[32] Muthukumaran, P.; Thiyagarajan, G.; Arun Babu, R.; Lakshmi, B.S. Raffinose from Costus Speciosus Attenuates Lipid Synthesis through Modulation of PPARs/SREBP1c and Improves Insulin Sensitivity through PI3K/AKT. *Chemico-Biological Interactions.* **2018**, *284*, 80–89.

[33] Liu, Y.; Chen, J.; Tan, Q.; Deng, X.; Tsai, P.-J.; Chen, P.-H.; Ye, M.; Guo, J.; Su, Z. Nondigestible Oligosaccharides with Anti-Obesity Effects. *J. Agric. Food Chem.* **2020**, *68*, 4–16.

[34] St‐Onge, M.; Salinardi, T.; Herron‐Rubin, K.; Black, R.M. A Weight‐Loss Diet Including Coffee‐Derived Mannooligosaccharides Enhances Adipose Tissue Loss in Overweight Men but Not Women. *Obesity* **2012**, *20*, 343–348.

[35] Zhao, C.; Wu, Y.; Liu, X.; Liu, B.; Cao, H.; Yu, H.; Sarker, S.D.; Nahar, L.; Xiao, J. Functional Properties, Structural Studies and Chemo-Enzymatic Synthesis of Oligosaccharides. *Trends in Food Science & Technology.* **2017**, *66*, 135–145.

[36] Kaaman, M.; Sparks, L.M.; Van Harmelen, V.; Smith, S.R.; Sjölin, E.; Dahlman, I.; Arner, P. Strong Association between Mitochondrial DNA Copy Number and Lipogenesis in Human White Adipose Tissue. *Diabetologia.* **2007**, *50*, 2526–2533.

[37] Puigserver, P.; Wu, Z.; Park, C.W.; Graves, R.; Wright, M.; Spiegelman, B.M. A Cold-Inducible Coactivator of Nuclear Receptors Linked to Adaptive Thermogenesis. *Cell*. **1998**, *92*, 829–839.

[38] Jornayvaz, F.R.; Shulman, G.I. Regulation of Mitochondrial Biogenesis. *Essays in Biochemistry.* **2010**, *47*, 69–84.

[39] Lu, R.; Ji, H.; Chang, Z.; Su, S.; Yang, G. Mitochondrial Development and the Influence of Its Dysfunction during Rat Adipocyte Differentiation. *Mol Biol Rep*. **2010**, *37*, 2173–2182.

[40] Fazzari, M.; Audano, M.; Lunghi, G.; Di Biase, E.; Loberto, N.; Mauri, L.; Mitro, N.; Sonnino, S.; Chiricozzi, E. The Oligosaccharide Portion of Ganglioside GM1 Regulates Mitochondrial Function in Neuroblastoma Cells. *Glycoconj J.* **2020**, *37*, 293–306.

[41] Feng, W.; Liu, J.; Wang, S.; Hu, Y.; Pan, H.; Hu, T.; Guan, H.; Zhang, D.; Mao, Y. Alginate Oligosaccharide Alleviates D‐galactose‐induced Cardiac Ageing via Regulating Myocardial Mitochondria Function and Integrity in Mice. *J Cellular Molecular Medi*. **2021**, *25*, 7157–7168.

[42] Leu, S.-Y.; Tsai, Y.-C.; Chen, W.-C.; Hsu, C.-H.; Lee, Y.-M.; Cheng, P.-Y. Raspberry Ketone Induces Brown-like Adipocyte Formation through Suppression of Autophagy in Adipocytes and Adipose Tissue. *The Journal of Nutritional Biochemistry.* **2018**, *56*, 116–125.

[43] Sidossis, L.; Kajimura, S. Brown and Beige Fat in Humans: Thermogenic Adipocytes That Control Energy and Glucose Homeostasis. *J. Clin. Invest.* **2015**, *125*, 478–486.

[44] Seale, P.; Conroe, H.M.; Estall, J.; Kajimura, S.; Frontini, A.; Ishibashi, J.; Cohen, P.; Cinti, S.; Spiegelman, B.M. Prdm16 Determines the Thermogenic Program of Subcutaneous White Adipose Tissue in Mice. *J. Clin. Invest.* **2011**, *121*, 96–105.

[45] Seale, P.; Bjork, B.; Yang, W.; Kajimura, S.; Chin, S.; Kuang, S.; Scimè, A.; Devarakonda, S.; Conroe, H.M.; Erdjument-Bromage, H.; et al. PRDM16 Controls a Brown Fat/Skeletal Muscle Switch. *Nature.* **2008**, *454*, 961–967.

[46] Seale, P.; Kajimura, S.; Yang, W.; Chin, S.; Rohas, L.M.; Uldry, M.; Tavernier, G.; Langin, D.; Spiegelman, B.M. Transcriptional Control of Brown Fat Determination by PRDM16. *Cell Metabolism.* **2007**, *6*, 38–54.

[47] Lun, W.; Zhou, J.; Bai, Y.; Che, Q.; Cao, H.; Guo, J.; Su, Z. Chitosan Oligosaccharide Activates Brown Adipose Tissue by Modulating the Gut Microbiota and Bile Acid Pathways Based on Faecal Microbiota Transplantation. *Journal of Functional Foods.* **2023**, *108*, 105731.

[48] Murakami, Y.; Ojima-Kato, T.; Saburi, W.; Mori, H.; Matsui, H.; Tanabe, S.; Suzuki, T. Supplemental Epilactose Prevents Metabolic Disorders through Uncoupling Protein-1 Induction in the Skeletal Muscle of Mice Fed High-Fat Diets. *Br J Nutr*. **2015**, *114*, 1774–1783.

[49] Price, N.L.; Gomes, A.P.; Ling, A.J.Y.; Duarte, F.V.; Martin-Montalvo, A.; North, B.J.; Agarwal, B.; Ye, L.; Ramadori, G.; Teodoro, J.S.; et al. SIRT1 Is Required for AMPK Activation and the Beneficial Effects of Resveratrol on Mitochondrial Function. *Cell Metabolism.* **2012**, *15*, 675–690.

[50] Fu, Y.; Luo, N.; Klein, R.L.; Garvey, W.T. Adiponectin Promotes Adipocyte Differentiation, Insulin Sensitivity, and Lipid Accumulation. *Journal of Lipid Research*. **2005**, *46*, 1369–1379.

[51] Garcia, D.; Shaw, R.J. AMPK: Mechanisms of Cellular Energy Sensing and Restoration of Metabolic Balance. *Molecular Cell.* **2017**, *66*, 789–800.

[52] Li, Y.; Xu, S.; Mihaylova, M.M.; Zheng, B.; Hou, X.; Jiang, B.; Park, O.; Luo, Z.; Lefai, E.; Shyy, J.Y.-J.; et al. AMPK Phosphorylates and Inhibits SREBP Activity to Attenuate Hepatic Steatosis and Atherosclerosis in Diet-Induced Insulin-Resistant Mice. *Cell Metabolism.* **2011**, *13*, 376–388.

[53] Ruderman, N.B.; Julia Xu, X.; Nelson, L.; Cacicedo, J.M.; Saha, A.K.; Lan, F.; Ido, Y. AMPK and SIRT1: A Long-Standing Partnership? *American Journal of Physiology-Endocrinology and Metabolism.* **2010**, *298*, E751–E760.

[54] Wongkrasant, P.A.; Pongkorpsakol, P.; Ariyadamrongkwan, J.; Meesomboon, R.; Satitsri, S.; Pichyangkura, R.; Barrett, K.E.; Muanprasat, C. Prebiotic Fructo-Oligosaccharide Promotes Tight Junction Assembly in Intestinal Epithelial Cells via an AMPK-Dependent Pathway. *Biomedicine & Pharmacotherapy*. **2020,** *129*, 110415.

[55] Muanprasat, C.; Wongkrasant, P.; Satitsri, S.; Moonwiriyakit, A.; Pongkorpsakol, P.; Mattaveewong, T.; Pichyangkura, R.; Chatsudthipong, V. Activation of AMPK by Chitosan Oligosaccharide in Intestinal Epithelial Cells: Mechanism of Action and Potential Applications in Intestinal Disorders. *Biochemical Pharmacology.* **2015**, *96*, 225–236.

[56] Liu, X.; Chhipa, R.R.; Nakano, I.; Dasgupta, B. The AMPK Inhibitor Compound C Is a Potent AMPK-Independent Antiglioma Agent. *Molecular Cancer Therapeutics.* **2014**, *13*, 596–605.

[57] Vucicevic, L.; Misirkic, M.; Kristina, J.; Vilimanovich, U.; Sudar, E.; Isenovic, E.; Prica, M.; Harhaji-Trajkovic, L.; Kravic-Stevovic, T.; Vladimir, B.; et al. Compound C Induces Protective Autophagy in Cancer Cells through AMPK Inhibition-Independent Blockade of Akt/mTOR Pathway. *Autophagy.* **2011**, *7*, 40–50.

[58] Dasgupta, B.; Seibel, W. Compound C/Dorsomorphin: Its Use and Misuse as an AMPK Inhibitor. In *AMPK*; Neumann, D., Viollet, B., Eds.; Methods in Molecular Biology; Springer New York: New York, NY, 2018; Vol. 1732, pp. 195–202 ISBN 978-1-4939-7597-6.